International Journal of Thermodynamics (IJoT)
ISSN 1301-9724 / e-ISSN 2146-1511
https://dergipark.org.tr/en/pub/ijot

Vol. 25 (No. 4), pp. 56-65, 2022
doi: 10.5541/ijot.1136615
Published online: December 1, 2022

Research Article

Thermodynamic Modeling of Liquid-Liquid Equilibrium in Ternary Systems with Biodiesel and Isolated Ester (Methyl Palmitate)

J.K.A. Bezerra[1*], M.R.A Andrade[2], E.R. Silva[2], L.J.N. Duarte [3], G.G. Medeiros[4], E.L. Barros Neto[2]

[1,2] Graduate Chemical Engineering Program, Federal University of Rio Grande do Norte (UFRN), RN, Brazil.
[3] Department of Petroleum Engineering, Federal University of Rio Grande do Norte (UFRN), RN, Brazil.
[4] Departament of Chemical Engineering, Federal University of Rio Grande do Norte (UFRN), RN, Brazil.
Email: [1*] jessycakn@hotmail.com

Received 29 June 2022, Revised 28 September 2022, Accepted 20 October 2022

Abstract

Liquid-liquid equilibrium data were measured and analyzed for two ternary systems (biodiesel + methanol + glycerol and methyl palmitate + methanol + glycerol). Biodiesel, produced by the conventional chemical route at 60 °C for 60 min, using methanol and soybean oil at a molar rate of 10:1 and potassium hydroxide concentration (KOH) of 1 wt% exhibited thermal decomposition at temperatures between 100 and 250 ºC, reaching mass loss of approximately 98.8%, confirming soybean oil conversion into biodiesel by gas chromatography and thermogravimetry. Tie line composition quality was verified using Othmer-Tobias and Hand correlation equations. The distribution and selectivity coefficients were calculated for the immiscibility regions. The experimental tie line data exhibited good correlation in the UNIQUAC and NRTL thermodynamic models. The biodiesel system displayed deviations of 0.66 and 0.53% for the UNIQUAC and NRTL models, respectively. In addition, the methyl palmitate system showed a 1.23 and 0.48% deviation for the UNIQUAC and NRTL model, respectively. The individual behavior of the main biodiesel esters , based on the UNIQUAC model parameters, demonstrated that the type of fatty acid does not interfere in model correlation, likely due to the similarity between their composition and properties.

Keywords**:** *Liquid-liquid equilibrium; methyl palmitate; biodiesel; UNIQUAC; NRTL; othmer-tobias correlation.*

1. Introduction

The production and indiscriminate use of fossil fuels should decline in the coming decades due to global warming caused by greenhouse gas emissions, which lead to serious climatic disorder. Diversification of the global energy matrix has broadened and strengthened renewable energies and biofuels aimed at combining energy safety with sustainable development [1,2]. Responding to the technical, economic and environmental challenges to diversify the biodiesel-producing processes, the scientific community has conducted extensive research on adding new raw materials and catalysts to the biodiesel production chain aimed at improving its performance and reducing greenhouse gas emissions by transforming an environmental liability into an energy asset [3,4].

Biodiesel is a feasible alternative to diesel owing to its similar properties and applications, without requiring changes to internal combustion engines [5]. It is superior to fossil fuels because of its biodegradable, sustainable and environmentally friendly nature. In addition, its cetane number is higher, it contains practically no sulfur or aromatics and 10-11% oxygen by weight, characteristics that help reduce hydrocarbon emissions, carbon compounds and gases such as sulfur dioxide (SO_2) and nitrogen oxide (NO_X) [6–9].

The conventional biodiesel production route is based on the transesterification reaction of vegetable oils/animal fats, in the presence of an alcohol and catalyst. Biodiesel composition is directly related to the raw material used, conversion rate of the transesterification reaction and separation process efficiency of the resulting products. The compounds commonly found in soybean-based biodiesel include the following fatty acid methyl esters (FAMEs): methyl palmitate, methyl stearate, methyl oleate and methyl linoleate [10]. On an industrial scale, biodiesel production generates multiple impurities, including large amounts of glycerol that may reach 10% of the total, far higher than the market demand for the reuse of this by-product in other processes [11]. In this respect, a number of studies seek ways to optimize the transesterification reaction and reinsert glycerol into new production chains, making the process more economically and environmentally efficient [12,13].

Biodiesel requires a high purity grade and must undergo rigorous purification to prevent traces of glycerol, water, catalyst or alcohol. These products are easily separated by forming two immiscible liquid phases: the heavy (glycerol) and light (biodiesel) phase. Alcohol is also divided into the two phases [14]. In this regard, understanding liquid-liquid equilibrium (LLE) is an indispensable tool to raise the conversion rate of the transesterification reaction with an increase in biodiesel selectivity [15]. On the other hand,

*Corresponding Author

thermodynamic modeling with the excessive use of Gibbs free energy levels, governed by the contribution of functional groups (UNIFAC) or the local composition theory (UNIQUAC, NRTL, among others), is important in predicting phase separation behavior [16–19].

In recent years, a number of studies on experimental data and and thermodynamic modeling involving systems containing biodiesel + glycerol + alcohols were reported in the literature. Nunes et al. [20] assessed experimental data to define miscibility regions and determine parameters for the UNIQUAC model, applying the liquid-liquid equilibrium of sunflower oil biodiesel – methanol – glycerol ternary systems. Bazooyar et al. [21] provided an accurate intelligent model for the behavior of biodiesel – alcohol – glycerol system phases, comparing it with activity models (UNIQUAC). Noriega and Narváez [22] correlated the UNIFAC model from experimental data in order to accurately describe and predict the liquid-liquid equlibrium of the systems involved in the biodiesel process. However, there are few studies on liquid-liquid equilibrium for ternary systems containing pure esters, including ethyl palmitate + ethanol + glycerol [23], methyl oleate + methanol + water [24]. Thus, experimental liquid–liquid equilibrium data of systems involving pure fatty acid esters (such as methyl palmitate) are scarce in the literature, requiring more robust and conclusive studies [25]. In this context, the present study aimed at promoting methylic biodiesel using commercial soybean oil in a homogeneous route with potassium hydroxide (KOH). In addition, the LLE data of the two ternary systems were obtained as follows: system 1 (biodiesel + glycerol + methanol) and system 2 (methyl palmitate + glycerol + methanol). Finally, the experimental data were validated by Othmer-Tobias [26] and Hand [27] correlations and fit to the NRTL and UNIQUAC thermodynamic models.

2. Materials and Methods

2.1 Raw Material

Soybean oil (Soya®), methyl alcohol (Dinâmica Química Contemporânea, 99.8%) and potassium hydroxide (KOH) (Ciavicco®, 88%) were used in the transesterification reaction to produce biodiesel. Methyl palmitate (Sigma-Aldrich, 97.0%) and glycerol (Dinâmica Química Contemporânea, 99.5%) were used only in the liquid-liquid equilibrium study.

.

2.2 Biodiesel Synthesis

The biodiesel was produced by the methyl transesterification reaction of soybean oil, using potassium hydroxide as catalyst. The reaction was performed at 60 °C for 60 min, using a methanol to oil molar ratio of 10:1 and KOH concentration of 1 wt.%. The biodiesel was then separated from glycerol, added with hydrochloric acid to neutralize the catalyst and then washed with distilled water. Next, the biodiesel was distilled to remove any trace of methanol and unreacted oil residue (diglycerides and monoglycerides) [28]. Product composition and the amount of methyl ester were determined using a gas chromatograph (GC) (GCMS-QP2020 - Shimadzu) under the following conditions: SH-Rtx-5MS column (length, 30 m; diameter, 0.25 mm); injector temperature 230 °C; column temperature: 90-160 °C (10 °C.min-1), 160-180 °C (2 °C.min-1) and 180-230 °C (4 °C.min-1); carrier gas: 1.0 mL.min-1 of helium and thermogravimetric analysis (TGA) using a Shimadzu DTG-60 analyzer, with a heating rate of 10 °C/min, ambient temperature up to 1000 °C and flow rate of 50 mL/min in a nitrogen atmosphere.

2.3 Isothermal Phase Diagrams

Ternary phase diagrams were constructed based on the mass titration method using visual observation via the cloud point, in line with the methodology developed by Evangelista Neto et al. [29]. The experimental points representing the miscibility curves were prepared using a base calculation of 10 g and placed in an equilibrium cell with magnetic agitation (Matoli, model 100M028). The operating temperature was controlled by circulating water in a thermostatized water bath (Solab, model SL-155), that is, 300.15 K for biodiesel and 308.15 K for methyl palmitate (MP), the latter selected based on the melting point of ester (303.15 K). The equilibrium lines were determined from the mass weight of the constituents, assuming a base calculation of 30 g, following a previously established ternary composition. Next, the samples were placed in an equilibrium cell under agitation for 3 h and then maintained at rest for 18 h for complete phase separation by decantation, similar to the study by Sena and Pereira [30]. Aliquots from each phase were collected to determine their mass fractions by measuring density in a digital densimeter (Anton Paar DMA 4500M). All measurements were performed in duplicate. Tie lines were used to determine the distribution (β) and selectivity (*S*) coefficients in order to quantify the extraction power of the solvent. The calcium of these parameters was determined by Equations (1), (2) and (3), where β_2 represents the distribution coefficient of methanol; β_3, the distribution coefficient of glycerol; *S*, the selectivity coefficient; w_{21}, the mass fraction of methanol in the biodiesel or MP-rich phase of glycerol; w_{23}, the mass fraction of methanol in the glycerol-rich phase; w_{33}, the mass fraction of glycerol in the glycerol-rich phase and w_{31}, the mass fraction of glycerol in the biodiesel or MP-rich phase.

$$\beta_2 = \frac{w_{21}}{w_{23}} \tag{1}$$

$$\beta_3 = \frac{w_{31}}{w_{33}} \tag{2}$$

$$S = \frac{\beta_2}{\beta_3} \tag{3}$$

2.4 Thermodynamic Models

The Othmer-Tobias [26] and Hand [27] correlations were applied to assess the thermodynamic consistency of the experimental LLE data observed by the tie lines. Model filling considered the mass fractions of the components in the glycerol and biodiesel or MP-rich phases, according to Equations (4) and (5), respectively, where w_{11} is the mass fraction of the biodiesel or MP in the biodiesel or MP-rich phase, *a*, the linear coefficient and *b*, the slope.

$$ln\left(\frac{1-w_{33}}{w_{33}}\right) = a + b\left(\frac{1-w_{11}}{w_{11}}\right) \tag{4}$$

$$ln\left(\frac{w_{23}}{w_{33}}\right) = a + b\left(\frac{w_{21}}{w_{11}}\right) \tag{5}$$

In addition, thermodynamic modeling is assessed by using excess Gibbs energy models, in order to establish the reliability of the experimental data. In this sense, Non-

Random Two Liquids (NRTL) and Universal Quasi-Chemical (UNIQUAC) thermodynamic models were assessed based on the behavior of the binary interaction parameters of the ternary systems (biodiesel + glycerol + methanol and methyl palmitate + glycerol + methanol)]. The regression parameters of the UNIQUAC and NRTL models were obtained by the objective function (OF) shown in Equation (6), where j, I, and k indicate the phase, component and tile line, respectively; M represents the number of tie lines; w^{exp}, experimental mass composition and w^{cal}, the mass composition. The binary interaction of parameters was determined using the TML computational tool [31].

$$OF = \sum_{k=1}^{M}\sum_{j=1}^{2}\sum_{i=1}^{3}\left[\left(w_{ijk}^{exp} - w_{ijk}^{cal}\right)^2\right] \quad (6)$$

To evaluate the accuracy of the two models, the root-mean-square deviation (RMSD) was calculated by Equation (7), where k, j, i, w^{exp} and w^{cal} are the same as expressed in Equation (6).

$$RMSD(\%) = 100x\left[\sum_{k=1}^{M}\sum_{j=1}^{2}\sum_{i=1}^{3}\frac{\left(w_{ijk}^{exp} - w_{ijk}^{cal}\right)^2}{6M}\right]^{\frac{1}{2}} \quad (7)$$

The van der Waals molecular volume (r) and molecular surface area (q), parameters of the UNIQUAC model, were determined by the sum of the individual terms of each subgroup in the molecule of each component, as established by Equations (8) and (9) [32], where i is the system component; k, group identification; $v_k^{(i)}$, the number of k subgroups of component i; R_k, the value of the UNIFAC group volume parameter and Q_k, the value of the UNIFAC surface parameter. In the case of biodiesel, the parameters were determined using the weighted average that considered the composition of the principal esters.

$$r_i = \sum_k v_k^{(i)} R_k \quad (8)$$

$$q_i = \sum_k v_k^{(i)} Q_k \quad (9)$$

3. Results and Discussion

3.1 Biodiesel Synthesis

Figure 1 presents the TGA curve obtained from the biodiesel produced in the transesterification reaction. The biodiesel TGA curve showed only one mass loss event, reaching 98.8%, between 150 and 250 ºC, which corresponds to the volatilization and/or decomposition of fatty acid methyl ester, according to the results obtained by Andrade et al. [28]. Freire et al. [33] evaluated the thermal decomposition of biodiesel obtained between 243 and 266 ºC, which indicated the volatilization and/or combustion of the esters, mainly ethyl oleate and ethyl linoleate, and total mass decomposition above 266 °C.

Table 1 shows the composition of distilled biodiesel, according to GC-MS analysis. The main compounds in the biodiesel are methyl linoleate, methyl oleate and methyl palmitate, as observed by [34]. According to [35], the main fatty acids present in soybean oil are linoleic (52.83%), oleic (25.85%), and palmitic (11.05%), and the biodiesel produced from soybean oil contains a larger amount of their esters.

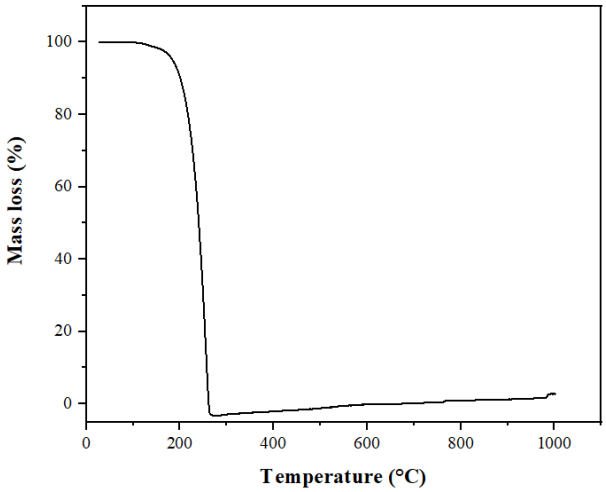

Figure 1. TGA curve of the distilled biodiesel.

Table 1. Biodiesel Composition.

Compound	Content %
Methyl caprate	2.93
Methyl laurate	4.74
Methyl palmitate	16.97
Methyl linoleate	42.69
Methyl oleate	27.36
Methyl stearate	5.02

3.2 Liquid-liquid Equilibrium

3.2.1 Ternary Diagrams

Knowledge of the biphasic region on a ternary diagram depends on the mutual solubility of the constituents present in the mixture, which must precede the implementation of the extraction or purification processes [18,36]. The miscibility curve (binodal) and tie line data of system 1 [biodiesel (1) + methanol (2) + glycerol (3)] and 2 [methyl palmitate (1) + methanol (2) + glycerol (3)] are presented in Tables 2 and 3 and plotted on the ternary diagrams of Figure 2.

Table 2. Experimental binodal curve data of the systems: [biodiesel (1) or MP (1)] + methanol (2) + glycerol (3).

Biodiesel (300.15 K)			Methyl Palmitate (308.15 K)		
w_1	w_2	w_3	w_1	w_2	w_3
0.07488	0.73697	0.18815	0.10046	0.71866	0.18087
0.03956	0.67011	0.29033	0.05238	0.66333	0.28429
0.02704	0.58028	0.39268	0.03195	0.57846	0.38958
0.01503	0.49122	0.49375	0.03169	0.48607	0.48224
0.01047	0.39438	0.59515	0.02506	0.38919	0.58574
0.00594	0.29722	0.69684	0.03541	0.28836	0.67623
0.00527	0.19831	0.79642	0.03543	0.19294	0.77163
0.00398	0.10069	0.89533	0.03995	0.09587	0.86418
0.18028	0.72000	0.09971	0.17475	0.69444	0.13081
0.28011	0.65186	0.06804	0.27364	0.63767	0.08870
0.38136	0.57215	0.04649	0.37461	0.56322	0.06216
0.48162	0.48210	0.03628	0.47958	0.48006	0.04036
0.58474	0.38936	0.02589	0.58063	0.38935	0.03002
0.69095	0.29595	0.01310	0.68456	0.29376	0.02168
0.79084	0.19822	0.01094	0.78582	0.19678	0.01740
0.88824	0.09974	0.01202	0.88237	0.09810	0.01954

Table 3. Phase equilibrium composition of the constituents.

Biodiesel-rich phase			Glycerol-rich phase		
w_1	w_2	w_3	w_1	w_2	w_3
Biodiesel (1) + methanol (2) + glycerol (3) at 300.15 K					
0.95030	0.03499	0.01471	0.00746	0.30918	0.68336
0.96835	0.01573	0.01592	0.00968	0.35745	0.63287
0.88841	0.09995	0.01163	0.02024	0.58708	0.39268
0.89162	0.09663	0.01175	0.05620	0.68287	0.26093
MP (1) + methanol (2) + glycerol (3) at 308.15 K					
0.89414	0.08829	0.01756	0.05783	0.65770	0.28446
0.90542	0.07465	0.01993	0.03473	0.57018	0.39509
0.92375	0.05071	0.02554	0.02026	0.34881	0.63094
0.93157	0.03941	0.02902	0.02977	0.22871	0.74152

The binodal curves (Figure 2) obtained with system 1 (containing biodiesel) and 2 (with MP) show similar behavior, consisting of an external biphasic zone due to the low miscibility of the constituents, indicating a large region favorable to the extraction process. This low miscibility is attributed to the fact that the polar molecules methanol and glycerol show no affinity for biodiesel because it is a mixture of nonpolar substances. This behavior was also observed in the *Sterculia striata* biodiesel + glycerol + ethanol [37] and soybean FAME + water + glycerol systems [17]. Analogously, the tie lines obtained here are similar in both systems, and their slopes demonstrate that methyl alcohol solubility in the biodiesel-rich (Figure 2a) and MP-rich phase (Figure 2b) is lower than in the glycerol-rich phase, indicating that a small amount of methanol and glycerol needs to be removed in the FAME-rich phase during biodiesel production via fatty acid esterification with methanol. The volume of the soluble component in the alcohol generally depends on its intermolecular strength [38]. With respect to the experimental points representing the two equilibrium phases of the tie lines, good agreement was observed with the respective binodal curves, ensuring the reliability of the equilibrium data obtained. These results corroborate the studies reported by Esipovich *et al.* [39], who assessed FAMEs + vegetable oil + methyl alcohol + FAMEs + glycerol + methyl alcohol ternary systems, and Asoodeh *et al.* [7] who evaluated linseed oil biodiesel + methanol + glycerol.

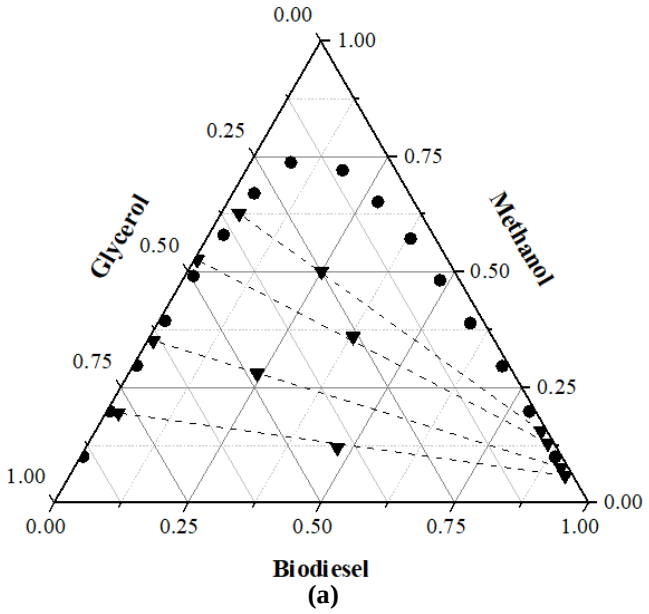

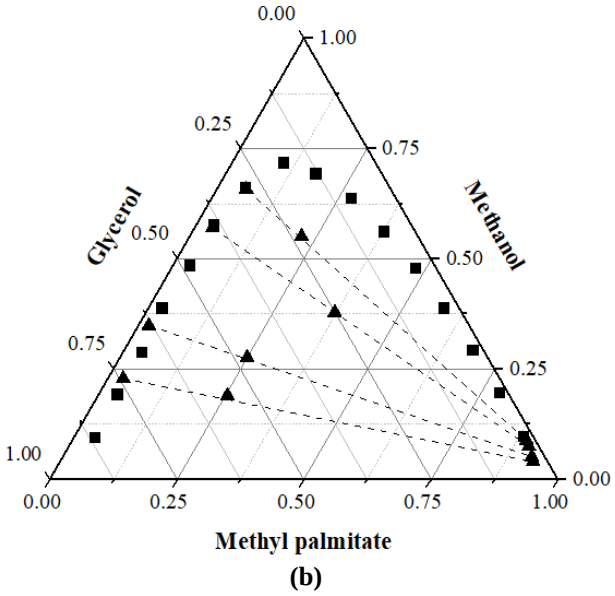

Figure 2. Ternary diagram for LLE of (a) system 1, with Biodiesel (1) + Methanol (2) + Glycerol (3) at 300.15 K (•) and (b) system 2, with Methyl palmitate (1) + Methanol (2) + Glycerol (3) at 308.15 K (■).

3.2.2 Distribution and Selectivity Coefficients

Liquid-liquid extraction, the selective transfer of a solute or impurity from a medium to a solvent, can be used in biodiesel purification to remove the glycerol obtained with the by-product in the transesterification reaction. The efficiency of biodiesel and MP extraction was assessed by the selectivity (S) and distribution coefficient (β). While selectivity indicates the capacity of the solvent to extract the solute without the need to extract other primary components from the solute, the distribution coefficient estimates the ability of the solvent to dissolve the solute, and can determine whether the number of extraction stages declines [40–42].

The distribution coefficients for systems 1 and 2, biodiesel and MP exhibited low values ($\beta_2 < 1$), indicating the preferential distribution of methanol in the glycerol-rich phase (Figure 3). The effect of the number of carbons in the FAME chain on the distribution coefficients of methanol remains unclear [43]. On the other hand, the distribution coefficients of methanol are smaller for MP than for biodiesel. A more marked decline was observed for system 1, given that it contains a mixture of methyl esters from longer and more saturated carbon chains than those of system 2. This behavior has a significant influence on the separation and purification stages involved in the optimization of methylic biodiesel, since higher distribution coefficients indicate a greater trend for biodiesel to absorb the solute (alcohol). Cavalcanti et al. [25] observed the same behavior in an LLE study for systems containing fatty acid, ethanol and glycerol ethyl esters. Analysis of the standard error of all experimental data showed that the value did not exceed 0.01, demonstrating dataset uniformity, indicating that the values obtained are concentrated around the mean.

Figure 4 shows that the selectivity values decline with an increase in the amount of methanol and are greater than one in all cases. This behavior demonstrates that most of the methanol is concentrated in the glycerol-rich phase, as confirmed by the tie lines in the LLE diagrams in Figure 2. However, selectivity values indicate a biodiesel-rich contamination phase and an increase in methyl ester

concentration in the glycerol-rich phase due to excess methanol [44,45]. This means that the cost of biodiesel purification rises owing to the higher amount of excess methanol and its effect on glycerol and biodiesel or MP distribution between the two phases. The results corroborate those reported by Melo et al. [46], who reported that the selectivity coefficients obtained were higher than 1, indicating that methanol is an excellent solvent for glycerin extraction in the biodiesel-rich phase.

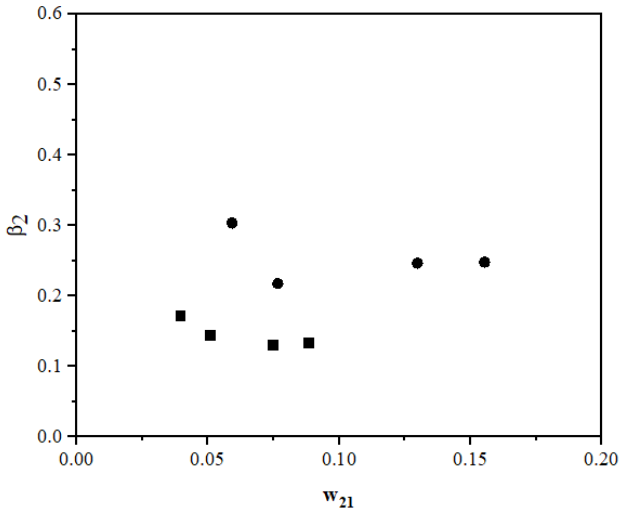

Figure 3. Experimental solute distribution coefficient (β_2) as a function of methanol mass fraction for system 1, with biodiesel (•) at 300.15 K, and system 2, with methyl palmitate (■) at 308.15 K.

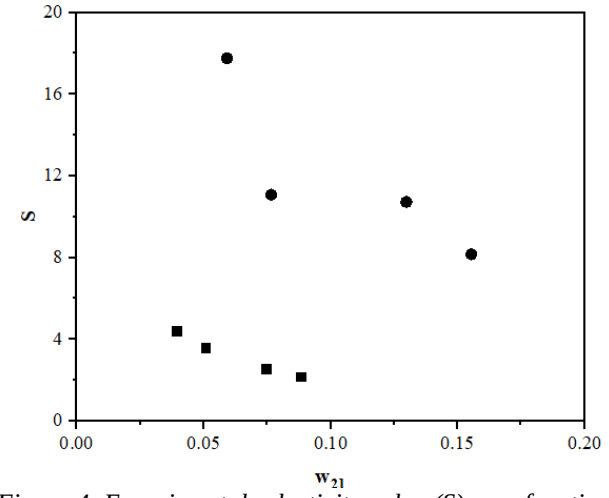

Figure 4. Experimental selectivity value (S) as a function of methanol mass fraction for system 1 (•) at 300.15 K, and system 2 (■) at 308.15 K.

3.3 Thermodynamic Models

3.3.1 Othmer-Tobias and Hand Correlations

The reliability of LLE experimental data, represented by the tie lines, was assessed by Othmer-Tobias and Hand correlations (Figure 5). These correlations can reproduce the tie lines using a straight line as a function of molar fractions [36,38]. Applying the Othmer-Tobias and Hand thermodynamic models to the experimental data obtained for the systems analyzed proved to be reliable and consistent, since they exhibited correlation coefficients above 0.97 (Table 4). Mousavi et al. [47] reported that the Othmer-Tobias and Hand correlations consistently represented the experimental equilibrium data of the systems containing glycerol + methanol + organic solvents.

Table 4. Othmer-Tobias and Hand and linear coefficient (R^2) for the systems studied.

Correlation	a	b	R^2
Biodiesel (1) + Methanol (2) + Glycerol (3)			
Othmer-Tobias	1.91225	3.70232	0.97314
Hand	1.72081	3.46989	0.97169
Methyl palmitate (1) + Methanol (2) + Glycerol (3)			
Othmer-Tobias	4.14445	9.78547	0.99941
Hand	2.37475	6.3189	0.99955

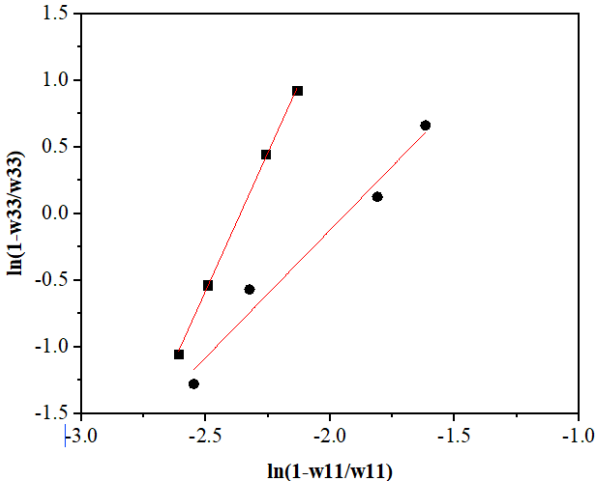

(a) Othmer-Tobias correlation

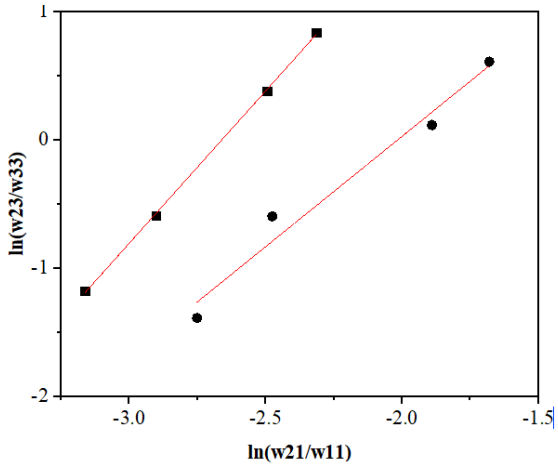

(b) Hand correlation

Figure 5. Thermodynamic consistency of the experimental data for system 1, with biodiesel (•) and system 2, with methyl palmitate (■).

3.3.2 NRTL and UNIQUAC Models

The structural q (van der Waals molecular surface area) and r parameters (van der Waals molecular volume) (Table 5) used for the UNIQUAC model were calculated from the contributions of the groups contained in the molecules of each component, in line with Prausnitz [32]. The binary interaction parameters of the UNIQUAC and NRTL models and parameter and non-randomness in a mixture (αij) were treated as adjustable parameters (Table 6). The root mean square deviation (RMSD) used to measure the accuracy of

the correlations was calculated from the difference between the experimental and calculated experimental mass (Table 6).

Table 5. The UNIQUAC structural parameters (r and q) for pure components.

Component	r	q
Biodiesel (Mix)	13.0726	10.7601
Methyl Oleate	13.3625	11.003
Methyl linoleate	13.1304	10.79
Methyl palmitate	12.2458	10.136
Methanol	1.4311	1.432
Glycerol	4.7957	4.908

Table 6. The binary parameters and the root mean square deviation (RMSD) of the Solvents (1) + Methanol (2) + Glycerol (3) ternary systems

Model	i-j	Aij	Aji	αij	RMSD (%)
Biodiesel (1) + Methanol (2) + Glycerol (3)					
UNIQUAC	1-2	2996.4	-311.8		
	1-3	-93.41	388.9		0.65952
	2-3	-85.932	654.33		
NRTL	1-2	2571.6	623.14	0.33632	
	1-3	824.9	946.37	0.20003	0.52932
	2-3	794.92	640.74	0.4472	
MP (1) + Methanol (2) + Glycerol (3)					
UNIQUAC	1-2	-1196.8	2532.8		
	1-3	-123.83	373.31		1.2319
	2-3	91.692	-148.54		
NRTL	1-2	747.88	-73.203	0.20206	
	1-3	781.03	920.07	0.27373	0.47579
	2-3	5736.7	995.66	0.26746	

Table 6 shows that both thermodynamic models correlated accurately with the experimental data for system 1, obtaining RMSD values below 0.66%. The NRTL model correlated the experimental data of system 2 more accurately than its UNIQUAC counterpart, obtaining an average RMSD of approximately 0.48% (NRTL) compared to 1.23% (UNIQUAC), similar to the studies conducted by [16,48]. The results presented in Table 6 can be visualized in Figures 6 (a) and (b), which show the fitting of the two models to the experimental data. In both systems (with biodiesel and MP), the NRTL model obtained smaller deviations, akin to the results presented by Rocha et al. [49], who obtained a good fit of this model to the experimental data of ternary systems with ethylic biodiesel from palm oil, obtaining an RMSD of 0.180% at 298.15 K for NRTL model. Do Carmo et al. [50] assessed four different thermodynamic models of activity coefficients that can be used for biodiesel in 34 different systems. The best results for NRTL and UNIQUAC models exhibited an RMSD of 9.1 and 8.2%, respectively, obtaining higher deviations than those presented here

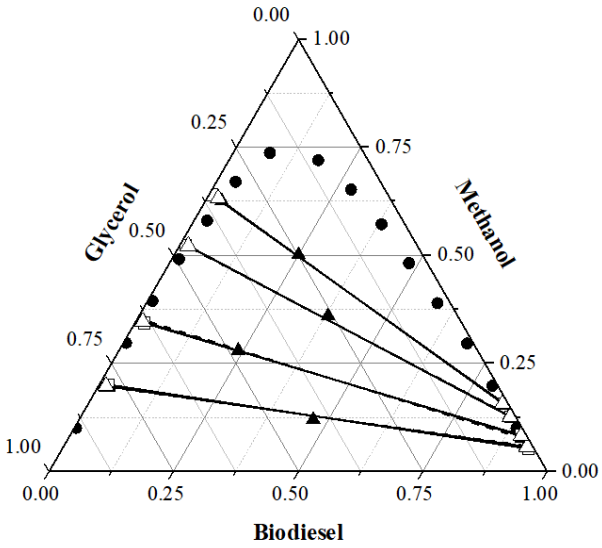

(a)

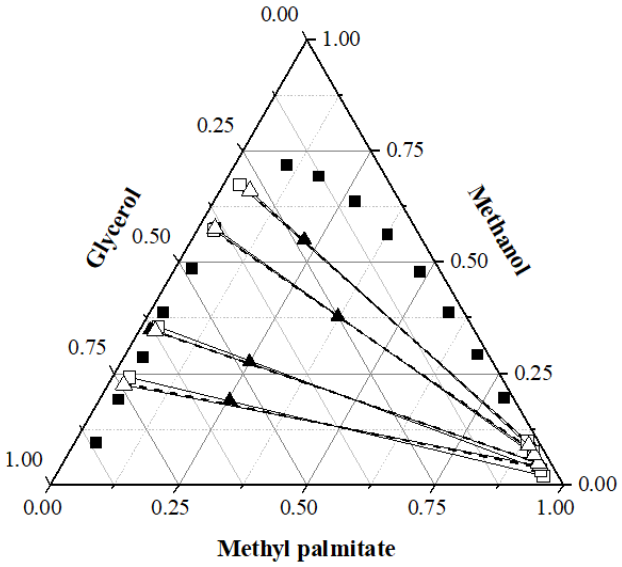

(b)

Figure 6. Ternary phase diagram for LLE of a) Biodiesel (1) + Methanol (2) + Glycerol (3) at 300.15 K (system 1) (•) and (b) Methyl palmitate (1) + Methanol (2) + Glycerol (3) at 308.15 K (system 2) (■). Experimental tie-line points (▲), NRTL model (Δ) and UNIQUAC model (□).

The UNIQUAC tie line parameters of system 1 were assessed in order to determine the best fit when applying the model and justify the difference in residual error. Figure 7 shows that any of the components can be selected to calculate the parameters and apply the model to the biodiesel. The components with the highest concentrations in biodiesel and a weighted average of the mixture were considered. All of these exhibited good fit to the experimental data. Lee et al. [51] found that methyl esters, methyl linoleate and methyl oleate in the presence of glycerol and methanol showed optimal results in terms of the experimental data fit to the UNIQUAC model. Mohadesi [52] reported that the UNIQUAC model is highly accurate considering the biodiesel (methyl ester), glycerol and methanol ternary system. Both studies demonstrate that the contributions of the subgroups contained in the molecules do not interfere in correlating the UNIQUAC model to the experimental data. Thus, the UNIQUAC model with optimized parameters

provides a reliable base to simulate separation of the FAME and glycerol-rich phases in biodiesel production processes.

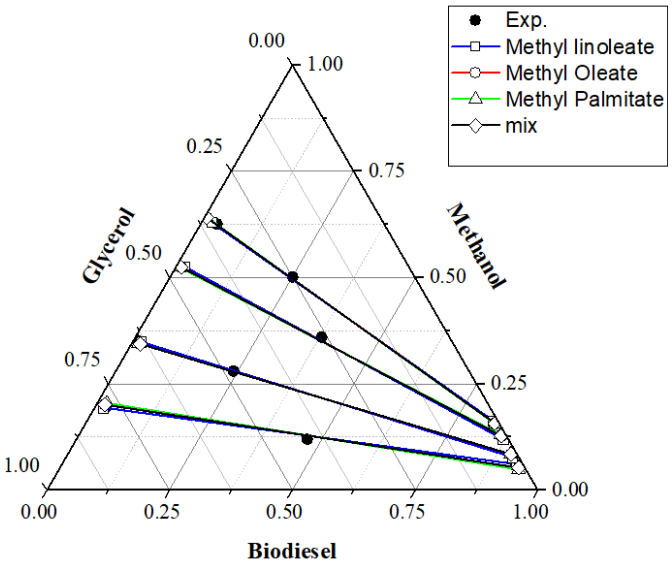

Figure 7. Experimental tie-line points for system 1: Biodiesel (1) + Methanol (2) + Glycerol (3) at 300.15 K and FAME parameters for the UNIQUAC model.

4. Conclusion

In the study of LLE, the solubility curves for system 1 (biodiesel + methanol + glycerol at 300.15K) and 2 (methyl palmitate + methanol + glycerol at 308.15 K) showed a curve with a large region of two phases. The tie lines constructed exhibited a marked decline, indicating good separation between biodiesel and the other components of system 1. Methanol content was higher in the glycerol-rich phase, resulting in important savings in the biodiesel purification stage. The study of equilibrium data consistency conducted using the Othmer-Tobias and Hand correlations show model fit, with R^2 values above 0.97. The Hand correlation exhibited better fit for both systems, confirming the good thermodynamic consistency of the experimental data. The UNIQUAC and NRTL thermodynamic models provided a good representation of experimental data, displaying an average square deviation of 0.66 and 0.53%, respectively for system 1. For system 2, the deviations were 1.23 and 0.48%, indicating better fit of the NRTL thermodynamic model. Assessment of UNIQUAC parameters, considering individual principal esters present in the biodiesel and a mixture of the respective esters, was conducted, showing that any of the components can be selected to calculate the parameters and apply the model to the biodiesel. The experimental data measured and presented in this study on pure biodiesel components and biodiesel system may be useful in building a database for researchers involved in biodiesel process development and optimization. The increasing diversification of the world energy matrix aims to combine energy security and sustainable development. For future research, the goal is to completely replace fossil fuel (diesel) with biodiesel and evaluate the effect of fuel on compression ignition engines in order to reduce carbon dioxide emissions and global warming.

Acknowledgments:

The authors are grateful to CAPES and the PPGEQ/DEQ/UFRN for their financial support.

Nomenclature

Symbol	*Variable*
β	*distribution coefficient*
S	*selectivity coefficient*
w^{exp}	*experimental mass composition*
w^{cal}	*mass composition*
r	*van der Waals molecular volume*
q	*molecular surface area*
v_k,	*the number of k subgroups*
R_k,	*UNIFAC group volume parameter*
Q_k,	*UNIFAC surface parameter.*

Subscripts

1	*Biodiesel or MP*
2	*Methanol*
3	*Glycerol*
j	*phase*
i	*component*
k	*tie lines*
M	*number of tie lines*

Abbrevations

LLE	*Liquid-Liquid Equilibrium*
MP	*Methyl palmitate*
GC	*Gas Chromatography*
OF	*Objective Function*
TGA	*Thermogravimetric analysis*
RMSD	*Root-mean-square deviation*
R^2	*Regression coefficient*

References

[1] T. Güney, "Renewable energy, non-renewable energy and sustainable development," *Int. J. Sustain. Dev. World Ecol.*, 26, 389–397, 2019, https://doi.org/10.1080/13504509.2019.1595214.

[2] P. Mukhopadhyay, R. Chakraborty, "LCA of sustainable biodiesel production from fried Borassus flabellifer oil in energy-proficient reactors: Impact assessment of multi fuel-additives on pour point, NOx and engine performance," *Sustain. Energy Technol. Assessments.*, 44, 100994, 2021, https://doi.org/10.1016/j.seta.2021.100994.

[3] J.A. Okolie, A. Mukherjee, S. Nanda, A.K. Dalai, J.A. Kozinski, "Next-generation biofuels and platform biochemicals from lignocellulosic biomass," *Int. J. Energy Res.*, 45, 14145–14169, 2021, https://doi.org/10.1002/er.6697.

[4] M. Viccaro, D. Caniani, S. Masi, S. Romano, M. Cozzi, "Biofuels or not biofuels? The "Nexus Thinking" in land suitability analysis for energy crops," *Renew. Energy.*, 187, 1050–1064, 2022, https://doi.org/10.1016/j.renene.2022.02.008.

[5] F. Fangfang, A. Alagumalai, O. Mahian, "Sustainable biodiesel production from waste cooking oil: ANN modeling and environmental factor assessment," *Sustain. Energy Technol. Assessments.*, 46, 101265, 2021, https://doi.org/10.1016/j.seta.2021.101265.

[6] M.M. Hasan, M.M. Rahman, "Performance and emission characteristics of biodiesel–diesel blend and environmental and economic impacts of biodiesel production: A review," *Renew. Sustain. Energy Rev.*, 74, 938–948, 2017,

https://doi.org/10.1016/j.rser.2017.03.045.

[7] A. Asoodeh, F. Eslami, S.M. Sadrameli, "Liquid–liquid equilibria of systems containing linseed oil biodiesel + methanol + glycerol: Experimental data and thermodynamic modeling," *Fuel.*, 253, 460–473, 2019, https://doi.org/10.1016/j.fuel.2019.04.170.

[8] M. Hashemzadeh Gargari, S.M. Sadrameli, "Investigating continuous biodiesel production from linseed oil in the presence of a Co-solvent and a heterogeneous based catalyst in a packed bed reactor," *Energy.*, 148, 888–895, 2018, https://doi.org/10.1016/j.energy.2018.01.105.

[9] J.C. Ge, S.K. Yoon, "Combustion and Emission Characteristics of a Diesel Engine Fueled with Crude Palm Oil Blends at Various Idling Speeds," *Applied Sciences*, 12(13), 6294, 2022.

[10] S.M. Rasulov, I.M. Abdulagatov, "PVT, saturated liquid density and vapor-pressure measurements of main components of the biofuels at high temperatures and high pressures: Methyl palmitate," *Fuel.*, 218, 282–294, 2018, https://doi.org/10.1016/j.fuel.2018.01.039.

[11] F. Yang, M.A. Hanna, R. Sun, "Value-added uses for crude glycerol - A byproduct of biodiesel production," *Biotechnol. Biofuels.*, 5, 1–10, 2012, https://doi.org/10.1186/1754-6834-5-1322413907.

[12] T. Zhang, C. Liu, Y. Gu, F. Jérôme, "Glycerol in energy transportation: A state-of-the-art review," *Green Chem.*, 23, 7865–7889, 2021, https://doi.org/10.1039/d1gc02597j.

[13] Y. Wang, Y. Muhammad, S. Yu, T. Fu, K. Liu, Z. Tong, X. Hu, H. Zhang, "Preparation of Ca-and Na-Modified Activated Clay as a Promising Heterogeneous Catalyst for Biodiesel Production via Transesterification," *Appl. Sci.*, 12, 2022, https://doi.org/10.3390/app12094667.

[14] C.S. Osorio-González, N. Gómez-Falcon, F. Sandoval-Salas, R. Saini, S.K. Brar, A.A. Ramírez, "Production of biodiesel from castor oil: A review," *Energies.*, 13, 1–22, 2020, https://doi.org/10.3390/en13102467.

[15] D.S. Negi, F. Sobotka, T. Kimmel, R. Schoma, "Liquid - Liquid Phase Equilibrium in Glycerol - Methanol - Methyl Oleate and Glycerol - Monoolein - Methyl Oleate Ternary Systems," *Ind. Eng. Chem. Res.*, 3693–3696, 2006.

[16] I.E.P. Toledo, L. Ferreira-Pinto, F.A.P. Voll, L. Cardozo-Filho, L. Meili, D.D.G. Coêlho, S.H.V. De Carvalho, J.I. Soletti, "Liquid-Liquid Equilibrium of the System {Peanut Biodiesel + Glycerol + Ethanol} at Atmospheric Pressure," *J. Chem. Eng. Data.*, 64, 2207–2212, 2019, https://doi.org/10.1021/acs.jced.8b01185.

[17] J.R.F. Silva, M.A. Mazutti, F.A.P. Voll, L. Cardozo-Filho, M.L. Corazza, M. Lanza, W.L. Priamo, J. Vladimir Oliveira, "Thermophysical properties of biodiesel and related systems: (Liquid + liquid) equilibrium data for Jatropha curcas biodiesel," *J. Chem. Thermodyn.*, 58, 467–475, 2013, https://doi.org/10.1016/j.jct.2012.10.006.

[18] T. Wannachod, M. Hronec, T. Soták, K. Fulajtárová, U. Pancharoen, A. Arpornwichanop, "Effects of salt on the LLE and tie-line data for furfuryl alcohol - N-butanol-water at T = 298.15 K," *J. Mol. Liq.*, 218, 50–58, 2016, https://doi.org/10.1016/j.molliq.2016.02.027.

[19] M. Maghami, J. Yousefi Seyf, S.M. Sadrameli, A. Haghtalab, "Liquid-liquid phase equilibrium in ternary mixture of waste fish oil biodiesel-methanol-glycerol: Experimental data and thermodynamic modeling," *Fluid Phase Equilib.*, 409, 124–130, 2016, https://doi.org/10.1016/j.fluid.2015.09.046.

[20] J.C. Nunes, J.J.P. Nascimento, A.S. Peiter, L. Ferreira-Pinto, J.I. Soletti, S.H.V. De Carvalho, J.J.N. Alves, A.C.B. De Araujo, "Experimental Data and Phase Equilibrium Modeling in Ternary and Pseudoquaternary Systems of Sunflower Oil for Biodiesel Production," *J. Chem. Eng. Data*., 64, 412–420, 2019, https://doi.org/10.1021/acs.jced.8b00276.

[21] B. Bazooyar, F. Shaahmadi, M.A. Anbaz, A. Jomekian, "Intelligent modelling and analysis of biodiesel/alcohol/glycerol liquid-liquid equilibria," *J. Mol. Liq.*, 322, 114972, 2021, https://doi.org/10.1016/j.molliq.2020.114972.

[22] M.A. Noriega, P.C. Narváez, "UNIFAC correlated parameters for liquid-liquid equilibrium prediction of ternary systems related to biodiesel production process," *Fuel.*, 249, 365–378, 2019, https://doi.org/10.1016/j.fuel.2019.03.124.

[23] L.A. Follegatti-Romero, M.B. Oliveira, F.R.M. Batista, E.A.C. Batista, J.A.P. Coutinho, A.J.A. Meirelles, "Liquid-liquid equilibria for ternary systems containing ethyl esters, ethanol and glycerol at 323.15 and 353.15 K," *Fuel.*, 94, 386–394, 2012, https://doi.org/10.1016/j.fuel.2011.09.020.

[24] M. Toikka, P. Kuzmenko, A. Samarov, M. Trofimova, "Phase behavior of the oleic acid – methanol – methyl oleate – water mixture as a promising model system for biodiesel production: Brief data review and new results at 303.15 K and atmospheric pressure," *Fuel.*, 319, 2022, https://doi.org/10.1016/j.fuel.2022.123730.

[25] R.N. Cavalcanti, M.B. Oliveira, A.J.A. Meirelles, "Liquid-liquid equilibria for systems containing fatty acid ethyl esters, ethanol and glycerol at 333.15 and 343.15 K: Experimental data, thermodynamic and artificial neural network modeling," *Brazilian J. Chem. Eng.*, 35, 819–834, 2018, https://doi.org/10.1590/0104-6632.20180352s20160267.

[26] D.F. Othmer, E. Tobias, "Tie Line Correlation," *Industrial and Engineering Chemistry*, 34, 6, 1942, https://doi.org/https://doi-org.ez18.periodicos.capes.gov.br/10.1021/ie50390a600.

[27] D.B. Hand, *Dineric distribution*, 1930, https://doi.org/https://doi.org/10.1021/j150315a009.

[28] M.R. de Almeida Andrade, C.B. Silva, T.K.O. Costa, E.L. de Barros Neto, J.M. Lavoie, "An experimental investigation on the effect of surfactant for the transesterification of soybean oil over eggshell-derived CaO catalysts", *Energy Convers. Manag. X.*, 11, 2021, https://doi.org/10.1016/j.ecmx.2021.100094.

[29] A.A. Evangelista Neto, J.C.C. Sobrinho, H.N.M. Oliveira, H.F.S. Freitas, F.F.M. Silva, E.L. Barros Neto, "Liquid-Liquid Equilibrium Data for the Pseudo-Ternary Biodiesel of Chicken Fat + Methanol + Glycerol," *Brazilian J. Pet. Gas.*, 12, 123–133, 2018, https://doi.org/10.5419/bjpg2018-0012.

[30] C.. Sena, S.R.C; Pereira, "Melon Seed Oil Utilization for Biodiesel Production and Analysis of Liquid-Liquid Equilibrium for the System Biodiesel+Methanol+Glycerin," *Environ. Prog. Sustain. Energy.*, 33, 676–680, 2014, https://doi.org/10.1002/ep.

[31] L. Stragevitch, *Equilíbrio Líquido-Líquido de Misturas de Não Eletrólitos*, 1997.

[32] B.E. Reid, Robert C.; Prausnitz, John M.; Poling, *The Properties of Gases and Liquids*, 4th ed., New York, 1987.

[33] L.M.S. Freire, T.C. Bicudo, R. Rosenhaim, F.S.M. Sinfrônio, J.R. Botelho, J.R. Carvalho Filho, I.M.G. Santos, V.J. Fernandes, N.R. Antoniosi Filho, A.G. Souza, "Thermal investigation of oil and biodiesel from jatropha curcas L.," *J. Therm. Anal. Calorim.*, 96, 1029–1033, 2009, https://doi.org/10.1007/s10973-009-0055-y.

[34] V. Kumbhar, A. Pandey, C.R. Sonawane, A.S. El-Shafay, H. Panchal, A.J. Chamkha, "Statistical analysis on prediction of biodiesel properties from its fatty acid composition," *Case Stud. Therm. Eng*., 30, 2022, https://doi.org/10.1016/j.csite.2022.101775.

[35] A. Alcántara-Carmona, F.J. López-Giménez, M.P. Dorado, "Compatibility studies between an indirect injection diesel injector and biodiesel with different composition: Stationary tests," *Fuel.*, 307, 2022, https://doi.org/10.1016/j.fuel.2021.121788.

[36] A. Ghanadzadeh Gilani, A. Najafgholizadeh, B. Mohammadi khanghah, M. Nasouri Gazani, "Experimental and correlational study of phase equilibria in aqueous solutions of phosphoric acid with alcohols at different temperatures," *J. Mol. Liq.*, 268, 553–560, 2018, https://doi.org/10.1016/j.molliq.2018.06.115.

[37] J.C.G. Filho, F.B. Bispo, M.L. Corazza, P.F. Arce, F.A.P. Voll, D. De Gusmão Coêlho, L. Ferreira-Pinto, S.H.V. De Carvalho, J.I. Soletti, "Liquid-Liquid Equilibrium Measurement and Thermodynamic Modeling of the { Sterculia striata Biodiesel + Glycerol + Ethanol} System," *J. Chem. Eng. Data.*, 66, 3293–3299, 2021, https://doi.org/10.1021/acs.jced.1c00341.

[38] Y. Jiang, S. Lin, H. Yan, H. Guo, Q. Li, "Liquid-liquid equilibrium data measurement and thermodynamic modelling for ternary mixtures composed of water, diethylene glycol dimethyl ether and different solvents at 298.2 K," *J. Chem. Thermodyn.*, 165, 0–7, 2020, https://doi.org/10.1016/j.jct.2021.106669.

[39] A.L. Esipovich, A.E. Rogozhin, A.S. Belousov, E.A. Kanakov, K. V. Otopkova, S.M. Danov, "Liquid–liquid equilibrium in the systems FAMEs + vegetable oil + methyl alcohol and FAMEs + glycerol + methyl alcohol," *Fuel.*, 217, 31–37, 2018, https://doi.org/10.1016/j.fuel.2017.12.083.

[40] A. Ghanadzadeh Gilani, J. Jahanbin sardroodi, F. Verpoort, S. Rahmdel, "Experimental study and thermodynamic modeling of phase equilibria of systems containing cyclohexane, alcohols (C4 and C5), and deep eutectic solvents," *J. Mol. Liq.*, 340, 2021, https://doi.org/10.1016/j.molliq.2021.117196.

[41] X. Meng, X. Liu, J. Gao, D. Xu, L. Zhang, Y. Wang, "Liquid-Liquid Equilibrium of Isobutyl Acetate + Isobutyl Alcohol + Imidazolium-Based Ionic Liquids at 298.15 and 308.15 K," *J. Chem. Eng. Data.* 64, 778–783, 2019, https://doi.org/10.1021/acs.jced.8b01045.

[42] M.P. Cumplido, A. Cháfer, J.I. Guayazan-Jaimes, J. de la Torre, J.D. Badia, "Potential of phosphonium-based ionic liquids to purify 1-propanol from water by liquid–liquid extraction at mild conditions," *J. Chem. Thermodyn.*, 165, 2022, https://doi.org/10.1016/j.jct.2021.106588.

[43] S. Shiozawa, D. Gonçalves, M.C. Ferreira, A.J.A. Meirelles, E.A.C. Batista, "Liquid-liquid equilibrium data and thermodynamic modeling of systems involved in the biodiesel production in terms of acylglycerols, free fatty acids, ethyl esters, and ethanol at 303.2 and 318.2 K and local pressure," *Fluid Phase Equilib.*, 507 112431, 2020, https://doi.org/10.1016/j.fluid.2019.112431.

[44] H. Liu, B. Jia, W. Sun, S. Dong, "Measurement and Thermodynamic Modeling of Ternary (Liquid + Liquid) Equilibrium for Extraction of 2-Methyl-3-buten-2-ol from Aqueous Solution with Different Solvents," *J. Chem. Eng. Data.*, 65, 5030–5036, 2020, https://doi.org/10.1021/acs.jced.0c00667.

[45] H. Shekaari, M.T. Zafarani-Moattar, B. Mohammadi, "Effective extraction of benzene and thiophene by novel deep eutectic solvents from hexane / aromatic mixture at different temperatures," *Fluid Phase Equilib.*, 484, 38–52, 2019, https://doi.org/10.1016/j.fluid.2018.11.025.

[46] K.R.B. De Melo, G.C. Lopes, D.D.G. Coêlho, J.I. Soletti, "Liquid-liquid equilibrium for systems composed by biodiesel from catolé oil (Syagrus cearensis), methanol and glycerol," *Chem. Ind. Chem. Eng. Q.*, 26, 21–29, 2020, https://doi.org/10.2298/CICEQ190508021B.

[47] H.S. Mousavi, M. Rahimi, M. Mohadesi, "Experimental Investigation and Thermodynamic Modeling of Glycerin/Methanol/Organic Solvent Systems," *Chem. Eng. Technol.*, 42, 628–636, 2019, https://doi.org/10.1002/ceat.201800356.

[48] L.R. Kanda, F.A.P. Voll, M.L. Corazza, "LLE for the systems ethyl palmitate (palmitic acid)(1)+ethanol(2)+glycerol (water)(3)," Fluid Phase Equilib. 354, 147–155, 2013, https://doi.org/10.1016/j.fluid.2013.06.027.

[49] E.G.D.A. Rocha, L.A. Follegatti-Romero, S. Duvoisin, M. Aznar, "Liquid-liquid equilibria for ternary systems containing ethylic palm oil biodiesel + ethanol + glycerol/water: Experimental data at 298.15 and 323.15 K and thermodynamic modeling," *Fuel.*, 128, 356–365, 2014,

https://doi.org/10.1016/j.fuel.2014.01.074.

[50] F.R. Do Carmo, N.S. Evangelista, R.S. De Santiago-Aguiar, F.A.N. Fernandes, H.B. De Sant'Ana, "Evaluation of optimal activity coefficient models for modeling and simulation of liquid-liquid equilibrium of biodiesel + glycerol + alcohol systems," *Fuel.* 125, 57–65, 2014, https://doi.org/10.1016/j.fuel.2014.01.108.

[51] M.J. Lee, Y.C. Lo, H.M. Lin, "Liquid-liquid equilibria for mixtures containing water, methanol, fatty acid methyl esters, and glycerol," *Fluid Phase Equilib.*, 20.299983.1309.

299 180–190, 2010, https://doi.org/10.1016/j.fluid.2010.10.010.

[52] M. Mohadesi, "Liquid-Liquid Equilibrium for Ternary Systems Containing Biodiesel + Glycerol + Alcohol (Ethanol or Methanol): Thermodynamic Modeling," *Journal of Chemical and Petroleum Engineering*, 54, 285–295, 2020, https://doi.org/10.22059/jchpe.20